# Drag Coefficients of Oceanographic Mooring Components

M. FINKE AND G. SIEDLER

*Institut für Meereskunde, Kiel University, 2300 Kiel, F.R.G.*

(Manuscript received 26 April 1985, in final form 2 September 1985)

ABSTRACT

The inclination of oceanographic mooring lines due to current drag causes errors in time series observations of currents and temperatures. The prediction of this effect requires knowledge of the drag coefficients for the mooring components. Drag coefficients, known for simple geometric shapes such as spheres or cylinders, are commonly used for mooring response computations. Selected mooring components (buoyancy elements and instruments) were tested in a tow tank to determine their actual drag coefficients. Over the Reynolds Number range, typical of oceanic conditions, deviations of the drag coefficient up to 50% are found when compared with the appropriate simple geometric shape coefficients. A set of model moorings and model current profiles is used to determine the resulting changes in component depth level and displacement. The changes in horizontal displacement of the upper part of the mooring are on the order of 10% in extreme cases and 1% under typical conditions. Their effects on current measurements will usually be negligible. However, the related vertical displacements are on the order 100 to 10 m. Such vertical displacements *may* carry instruments to depth levels where currents and particularly thermocline temperatures are sufficiently different from the intended level to cause errors in the time series observations.

## 1. Introduction

Oceanographic moorings are composed of instruments, cables, buoyancy elements and auxiliary equipment such as acoustic releases, radio beacons, etc. Mooring design requires finding the appropriate compromise between the goal of keeping the mooring line straight in the vertical and the requirement of minimizing cable diameters and total buoyancy. With reasonable choices of cables and buoyancy it has to be accepted that forces due to current drag will cause a non-negligible inclination of the mooring line (Fofonoff, 1969). A knowledge of the degree of inclination is required to estimate errors in time series observations due to the resulting instrument displacements. A sufficiently exact determination of the drag forces is needed for predicting the mooring performance and for selecting the appropriate mooring configuration (Casarella and Parsons, 1970).

The drag force can be written as

$$F = \frac{1}{2} C_D \rho A V^2 \tag{1}$$

where

| | |
|---|---|
| $F$(N) | drag force |
| $C_D$ | drag coefficient |
| $\rho$ (kg m$^{-3}$) | mass density of the fluid |
| $A$ (m$^2$) | cross-sectional area |
| $V$ (m s$^{-1}$) | relative velocity. |

The drag coefficient is a characteristic dimensionless number for a body in the flow field, depending on the Reynolds number Re and the direction of the current with respect to a specified body axis:

$$C_D = \frac{2F}{\rho A V^2} = f(\mathrm{Re}, \alpha) \tag{2}$$

where

| | | |
|---|---|---|
| $\mathrm{Re} = Vd/\nu$ | Reynolds number, | (3) |
| $d$ (m) | characteristic length, | |
| $\nu$ (m$^2$ s$^{-1}$) | kinematic viscosity, | |
| $\alpha$ | angle between flow direction and specified body axis. | |

When there is no tilt, $\alpha$ is zero.

Since cables, instrument housings and buoyancy elements have shapes which approximately resemble cylinders, spheres or other simple geometric forms, the drag coefficients for mooring components are usually assumed to be those of the corresponding bodies with a simple shape for the appropriate range of Reynolds numbers. Their data are available in mechanical or ocean engineering handbooks (e.g., Sass and Bouché, 1956; Hoerner, 1965; Myers et al., 1969). In the case of deep-sea moorings, cable drag presents the largest portion of the overall drag forces because of the large cross-sectional area ($A$), and drag coefficients have been determined experimentally for some cables (e.g., Berteaux, 1976). Although the errors in the selected drag coefficients for other mooring components will be less important because of smaller $A$, they may well lead to significant errors in predicted mooring line inclinations and instrument depths. Buoyancy elements and instruments are often concentrated in the upper part of

the mooring configuration. Drag force changes will be more effective there in causing displacements because of the mooring geometry and because of stronger currents in the upper layer (Fofonoff, 1969).

It was therefore decided to determine the drag coefficients of selected mooring components that are commonly used in oceanographic laboratories, including a special buoyancy element that is part of most moorings of the Institut für Meereskunde (IfM) at Kiel University. It will be shown from tow tank results that major deviations from the $C_D$ of corresponding bodies with simpler geometry occur in some cases, and that predictions of mooring performance can be significantly affected.

## 2. The tested mooring components

The components selected for the tow tank measurements are shown in Fig. 1, and the information on the geometry is presented in Table 1.

(i) K450, Kiel 450 Kilogram Float: Synthetic foam buoyancy element, ellipsoidal form. Material: Divinicell, manufacturer Diab Baracuda/Sweden. Comment: This is a subsurface float used by IfM as a top element in moorings, with additional radio beacon and light installed. Compared to steel or aluminium spheres, these floats are less susceptible to excessive pressure during launching and are also fairly stable in surface waves during recovery.

(ii) K320, Kiel 320 Kilogram Float: Synthetic foam buoyancy element, ellipsoidal form. Material: Divinicell, manufacturer Diab Baracuda/Sweden.

(iii) B1, Benthos 2-Ball Float: Pair of deep-sea glass spheres in hardhats (Benthos, type 204 HR-17) connected by chain links (IfM).

(iv) B2, Benthos 2-Ball Buoyancy: Pair of deep-sea glass spheres in hardhats (Benthos, type 204 HR-17) assembled in a frame (IfM) to be used as a surface float in recovery operations.

(v) TR 1, Temperature Recorder: Thermistor Cable Recorder, type TR 1. Manufacturer: Aanderaa/Norway.

(vi) RCM 4, Recording Current Meter: Current Meter, type RCM 4. Manufacturer: Aanderaa/Norway.

While the original components 3 to 6 could be towed directly, components 1 and 2 had to be reduced in size for the available tank. Table 1 summarizes the geometry of all components in full and reduced size.

When towing reduced-size models, the towing speed has to be adapted to conform with the necessary range of Reynolds numbers. With $\nu = 1.8 \times 10^{-2}$ to $0.6 \times 10^{-2}$ m$^2$ s$^{-1}$ in the temperature range $-2$ to 38°C and a current speed range from $10^{-2}$ to 1 m s$^{-1}$, the following approximate Reynolds number ranges are obtained from the values of $d$ in Table 1:

| | |
|---|---|
| K450, K320 (Kiel Floats) | $6 \times 10^3$–$2 \times 10^6$ |
| B1, B2 (Benthos Float/Buoyancy) | $2 \times 10^3$–$8 \times 10^5$ |
| TR 1, RCM 4 (Recorders) | $7 \times 10^2$–$2 \times 10^5$. |

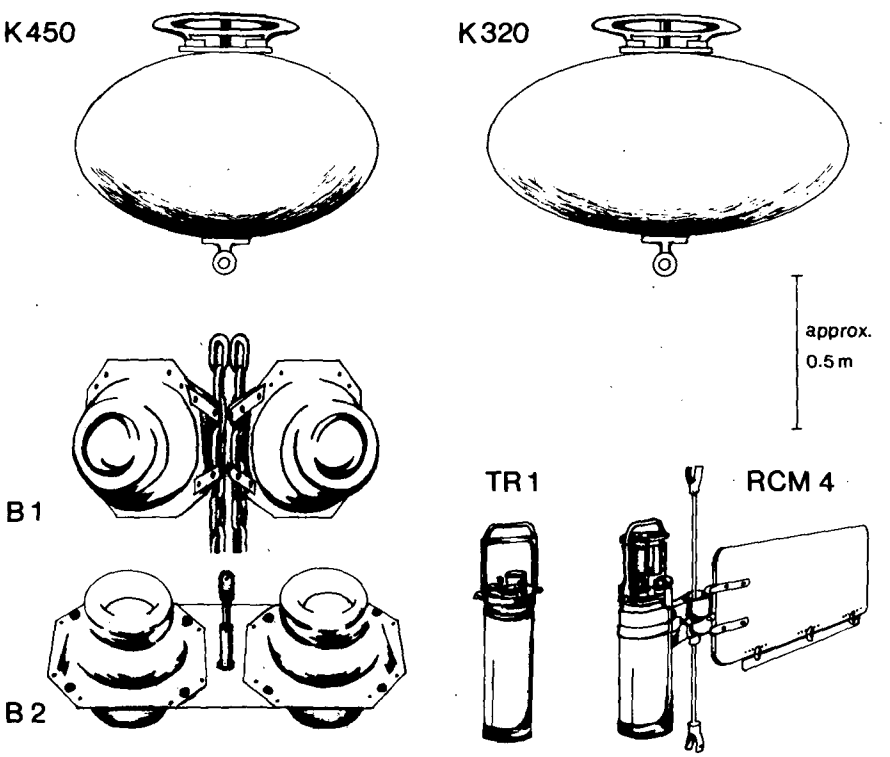


FIG. 1. The tested mooring components.

TABLE 1. Geometry of tested components: length in current direction, width, height and cross-sectional area normal to current direction.

| Number | Component | Length (m) | Width (m) | Height (m) | Cross-sectional area ($m^2$) |
|---|---|---|---|---|---|
| 1 | K450 original | 1.20 | 1.20 | 0.60 | 0.56 |
| 1 | K450 model | 0.36 | 0.36 | 0.18 | 0.051 |
| 2 | K320 original | 1.03 | 1.03 | 0.66 | 0.52 |
| 2 | K320 model | 0.28 | 0.28 | 0.18 | 0.040 |
| 3 | B1 | 0.44 | 0.90 | 0.48 | 0.45 |
| 4 | B2 | 0.48 | 0.90 | 0.44 | 0.35 |
| 5 | TR 1 | 0.13 | 0.13 | 0.68 | 0.043 |
| 6 | RCM 4 housing | 0.13 | 0.13 | 0.68 | 0.043 |

The towing speed has to be increased in the case of the reduced models to observe at the appropriate Reynolds numbers. The following ranges of Re were used in the tow tank experiments (20°C):

K450 (Kiel 450 kg float) $2.8 \times 10^4$–$8.3 \times 10^5$

K320 (Kiel 320 kg float) $2.8 \times 10^4$–$5.1 \times 10^5$

B1, B2 (Benthos float/buoyancy)

$5.0 \times 10^4$–$3.2 \times 10^5$

TR 1 (Temperature recorder)

$8.2 \times 10^3$–$2.6 \times 10^5$

RCM 4 (Recording current meter)

$1.1 \times 10^4$–$2.6 \times 10^5$

Experimental conditions thus correspond to a large range of typical oceanic current speeds for K450, K320, B1, B2 and to strong currents for TR 1 and RCM 4.

## 3. Experimental methods

The tow tank had the following dimensions: width 2.1 m, height 1.1 m, and length 35 m. The water depth was 1.0 m, resulting in a cross-sectional area of 2.1 $m^2$. Rails on top of the tank guided a carriage to which the tested components were attached. The speed of the carriage could be controlled over the range 0.05 to 2.7 m $s^{-1}$. After acceleration the carriage velocity was constant for a 10 m distance, with the speed measured by two light barriers and a quartz clock. Water temperature was monitored during the tests.

Forces were measured by a three-component balance mounted on the carriage. The bodies tested were attached to the carriage through a steel rod of 24 mm diameter and with a length adjusted for the individual bodies to be placed at mid-depth of the tank. The rod was shielded by a streamlined cover to reduce the drag on the supporting device, with a 5 cm distance between the cover and the body to be tested. The ratio of forces due to the drag on all the submerged parts and on the supporting device alone is shown in Fig. 2 for the case of K450 and K320 (Kiel Floats) models. The drag on the supporting device has to be considered in evaluating the data.

Measurement procedures included 1) the testing and calibration of the balance before and after the tows, 2) measurements of forces for each mooring component

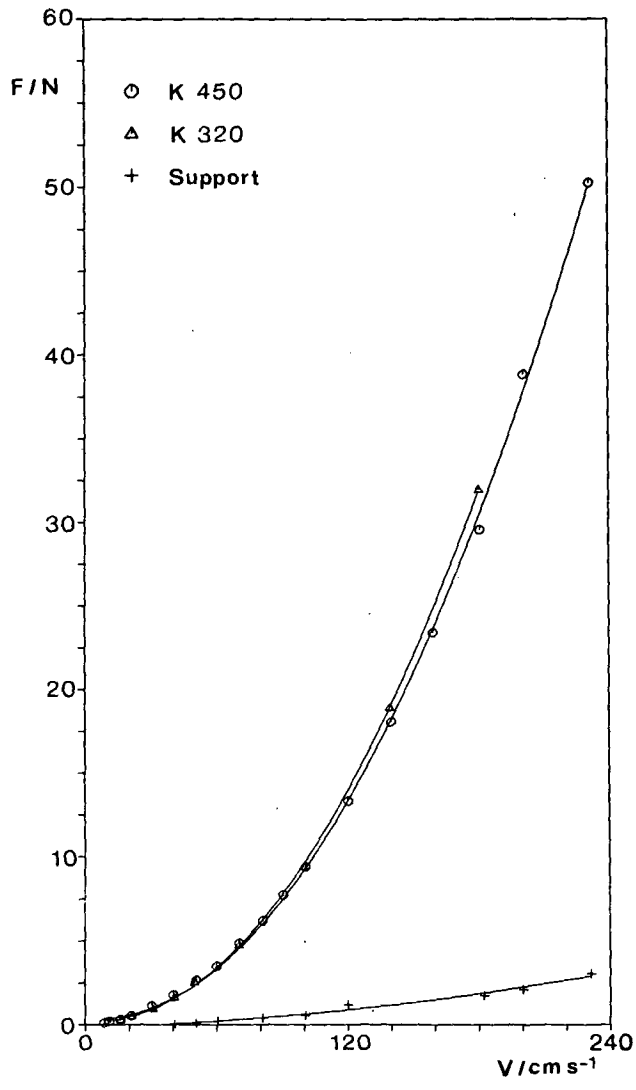


FIG. 2. Drag force $F$ on the Kiel 450 kg float (K450, circles) and the Kiel 320 kg float (K320, triangles) including the drag on the supporting device and drag forces on the supporting device alone (crosses).

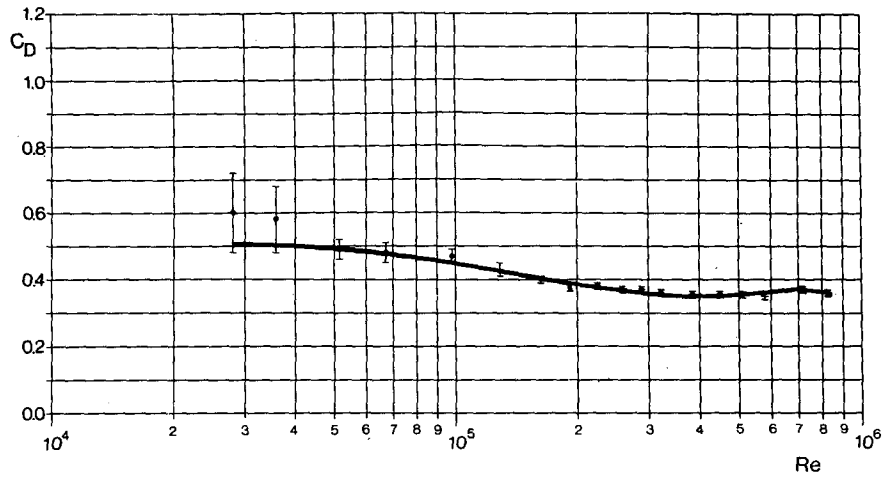


FIG. 3. Least squares fit of drag coefficient $C_D$ as a function of Reynolds number Re for the Kiel 450 kg Float (K450). Error bars indicate standard deviations.

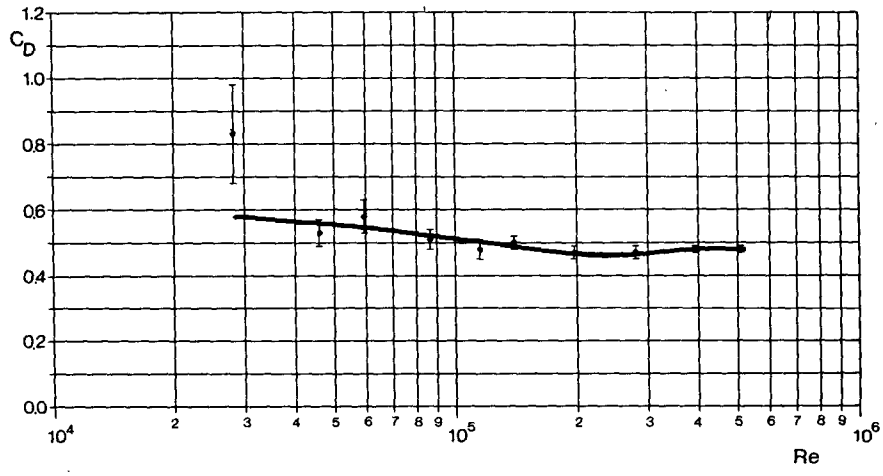


FIG. 4. As in Fig. 3 but for the Kiel 320 kg Float (K320).

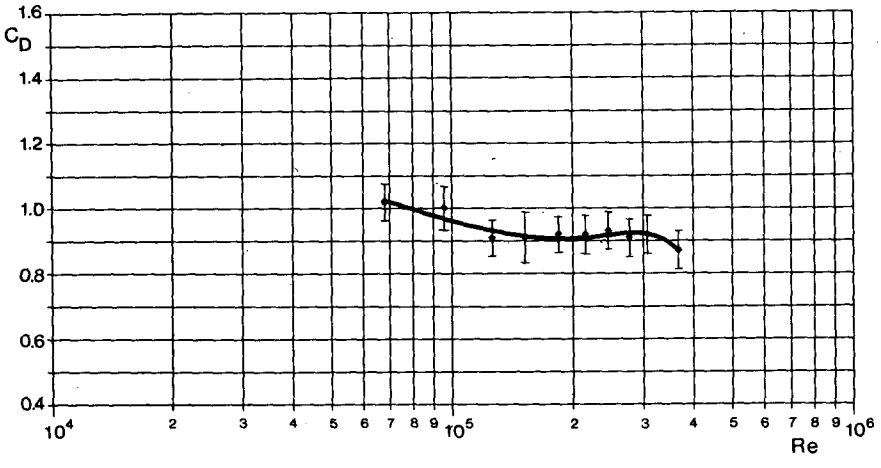


FIG. 5. As in Fig. 3 but for the Benthos 2-ball float (B1).

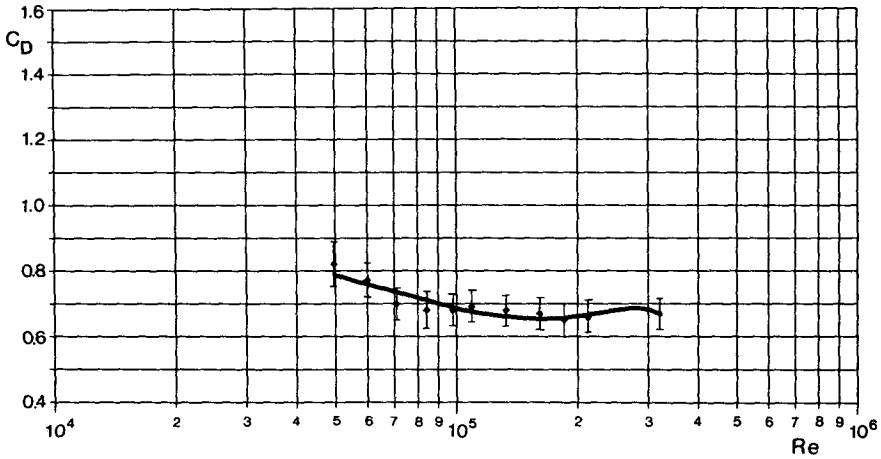


FIG. 6. As in Fig. 5 but for the Benthos 2-ball buoyancy float (B2).

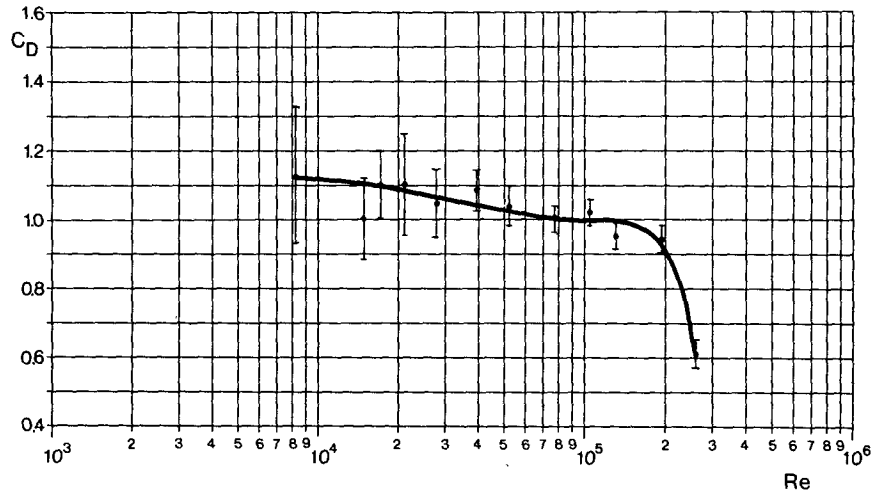


FIG. 7. As in Fig. 5 but for the temperature recorder TR 1.

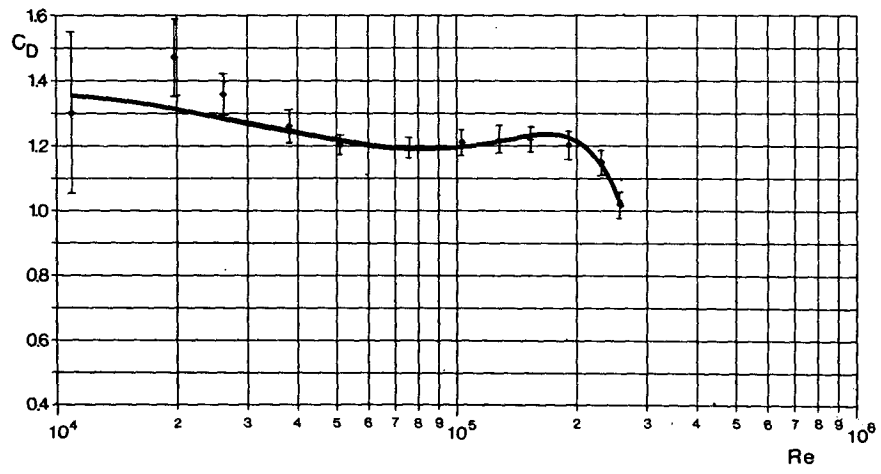


FIG. 8. As in Fig. 5 but for recording current meter RCM 4.

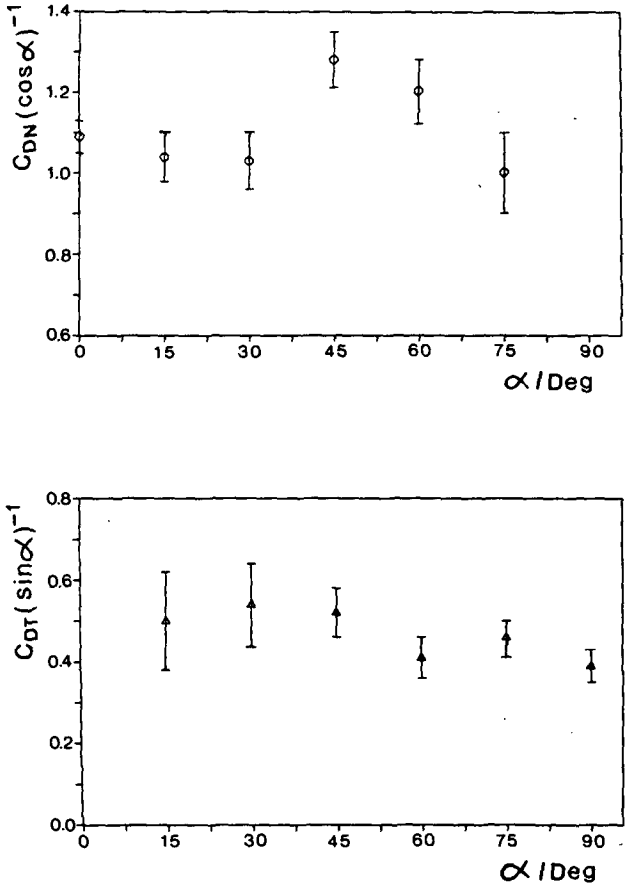


FIG. 9. Coefficients for normal ($C_{DN}$) and tangential ($C_{DT}$) drag according to Eqs. (6) and (7) as a function of instrument inclination $\alpha$, normalized by $\cos\alpha$ and $\sin\alpha$, respectively, for the temperature recorder (TR 1) at Re = $5.2 \times 10^4$.

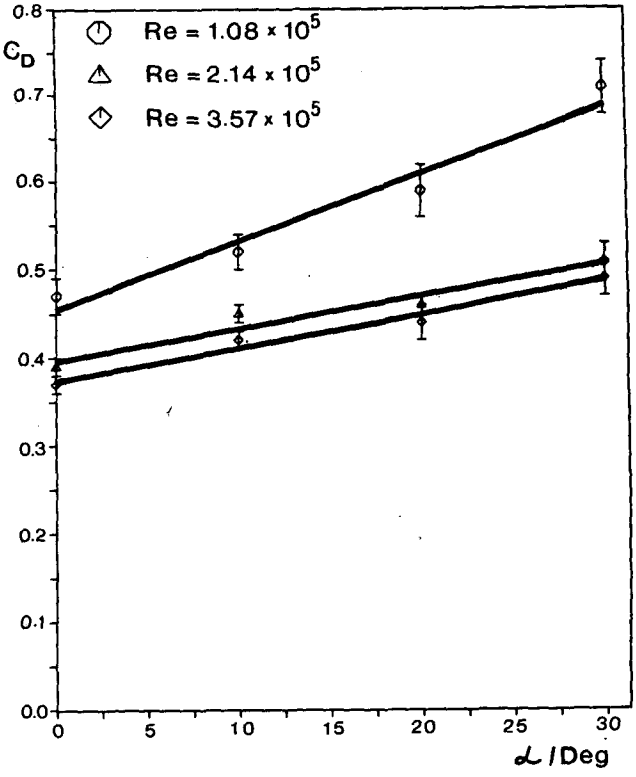


FIG. 10. Drag coefficient $C_D$ according to Eq. (2) as a function of component inclination $\alpha$ and selected Re for the Kiel 450 kg float (K450).

at selected speeds, 3) measurements of forces for selected angles of attack with components K450 (Kiel 450 kg Float) and TR 1 (Temperature Recorder) and 4) measurements with a standard cylinder for intercomparison.

Errors can be determined from

$$\frac{\Delta C_D}{C_D} = \left[\left(\frac{\Delta F_x}{F_x}\right)^2 + \left(\frac{\Delta\rho}{\rho}\right)^2 + 2\left(\frac{\Delta V}{V}\right)^2\right]^{1/2} \quad (4)$$

where $\Delta C_D$, $\Delta F_x$, $\Delta\rho$ and $\Delta V$ are the deviations of the drag coefficient $C_D$, the along-channel force component $F_x$, the density $\rho$ and the speed $V$. With $\Delta V \approx \pm 10^{-4}$ m s$^{-1}$ and with $\Delta\rho \approx \pm 10^{-1}$ kg m$^{-3}$ for a temperature variation of $\Delta T = \pm 0.1$°C, $\Delta V/V$ and $\Delta\rho/\rho$ are found to be 1–2 orders of magnitude below $\Delta F_x/F_x$, and the error in $C_D$ is therefore given to a good approximation by

$$\Delta C_D = C_D \frac{\Delta F_x}{F_x}. \quad (5)$$

Details on measurement procedures and the error analysis are given by Finke (1984). The typical overall relative error is about ±3% for the Kiel Floats K450 and K320, and the recorders TR 1 and RCM 4, and about ±6% for the Benthos Float B1 and the Benthos

TABLE 2. Comparison of drag coefficients for mooring components tested and for similar bodies with simple geometry.

| Mooring component tested | Similar body with simple geometry | $\frac{C_D(\text{comp}) - C_D(\text{body})}{C_D(\text{body})} \times 100$ |
|---|---|---|
| K450 Kiel 450 kg float | Sphere | −22% |
| K320 Kiel 320 kg float | Sphere | +6 |
| B1 Benthos 2-ball float | Spheres | +52 |
| B2 Benthos 2-ball buoyancy | Spheres | +14 |
| TR 1 Temperature recorder | Cylinder (1:15) | +14 |
| RCM 4 Recording current meter | Cylinder (1:5) | +35 |

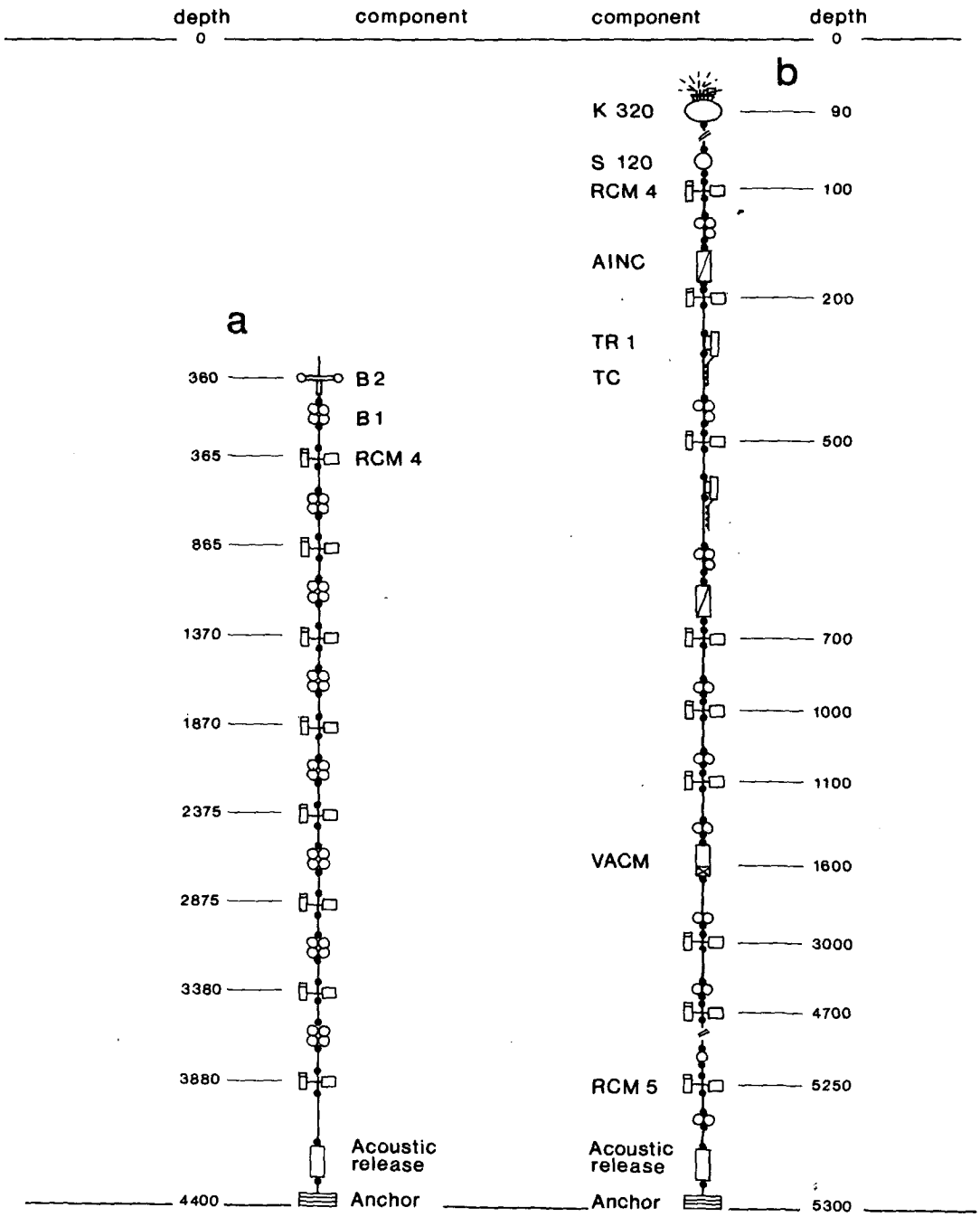


FIG. 11. Configuration of moorings M1 (a) and M4 (b), with tested components K320, B1, B2, TR 1 and RCM 4, and additional nontested components. S120: Buoyancy sphere with 1 m diameter, AINC: Inclination meter, TC: Thermistor cable, RCM 5: Current meter for large depths, VACM: Vector averaging current meter, and Acoustic release.

Buoyancy B2. Individual errors are indicated in the graphical presentations of results.

## 4. Results of tow tank experiments

The drag coefficients $C_D$ obtained from the tow tank experiments with zero angle of attack are shown as a function of Reynolds number in Figs. 3–8, including error intervals. It is well known in hydrodynamics that for bodies of round shapes such as spheres and cylinders, a critical Reynolds number exists where $C_D$ drops to a lower value. This is due to the downstream movement of the boundary layer separation point along the body's surface in the case of a turbulent boundary layer.

TABLE 3. Speed profiles assumed for mooring performance computations.

| Profile I | | | | Profile II | | Profile III | |
|---|---|---|---|---|---|---|---|
| M1 Depth (m) | M2 Depth (m) | M3 Depth (m) | Speed (cm $s^{-1}$) | Depth (m) | Speed (cm $s^{-1}$) | Depth (m) | Speed (cm $s^{-1}$) |
| 0 | 0 | 0 | 40 | 0 | 28 | 0 | 40 |
| 4400 | 440 | 176 | 0 | 1000 | 20 | 245 | 40 |
| | | | | 1500 | 17 | 550 | 50 |
| | | | | 2000 | 12.5 | 755 | 65 |
| | | | | 3000 | 0 | 1160 | 35 |
| | | | | 4400 | 0 | 1665 | 6 |
| | | | | | | 1760 | 6 |
| | | | | | | 3020 | 5 |
| | | | | | | 5300 | 0 |

For sharp-edged bodies the separation point is fixed, and there is a tendency to constant $C_D$ values over a larger range of Reynolds numbers (Prandtl, 1969). A typical range for the drop in the drag coefficient, due to this effect, is $3 \times 10^5$ to $5 \times 10^5$ (Sigloch, 1982), depending mainly on the character of the flow field and the roughness of the body's surface. The curves in Figs. 7 and 8 indicate the drop of $C_D$ in the expected range of Reynolds numbers for the temperature recorder and current meter. The critical Reynolds number is not reached in our measurements in the other cases presented in Figs. 3 to 6. The levels of $C_D$ for Reynolds numbers below the critical value are found to deviate from those of bodies with simple geometric shape. The most important deviations are those of the Benthos glass spheres (B1 and B2) because large numbers of such spheres are usually included in deep-sea moorings. The increase of $C_D$ by about 50% for the Benthos 2-ball float B1 is apparently caused by the deviations from a spherical shape due to the plastic hardhats and the frame with sharp edges. A corresponding increase of $C_D$ can be expected in glass ball tandem configuration with similar hardhats.

With the mooring bending over due to current forcing, mooring components may be inclined from the vertical. The change of drag forces due to a non-zero angle of attack was determined for the Kiel 450 kg Float K450 and the temperature recorder TR 1. In such cases drag forces are composed of normal and tangential components. For cables the normal and tangential drag forces are commonly assumed to be proportional to the square of the normal and tangential velocity components, respectively, with corresponding drag coefficients $C_{DN}$ and $C_{DT}$ taken constant and independent of the angle to flow direction (Choo and Casarella, 1971). The tangential drag force is small. In

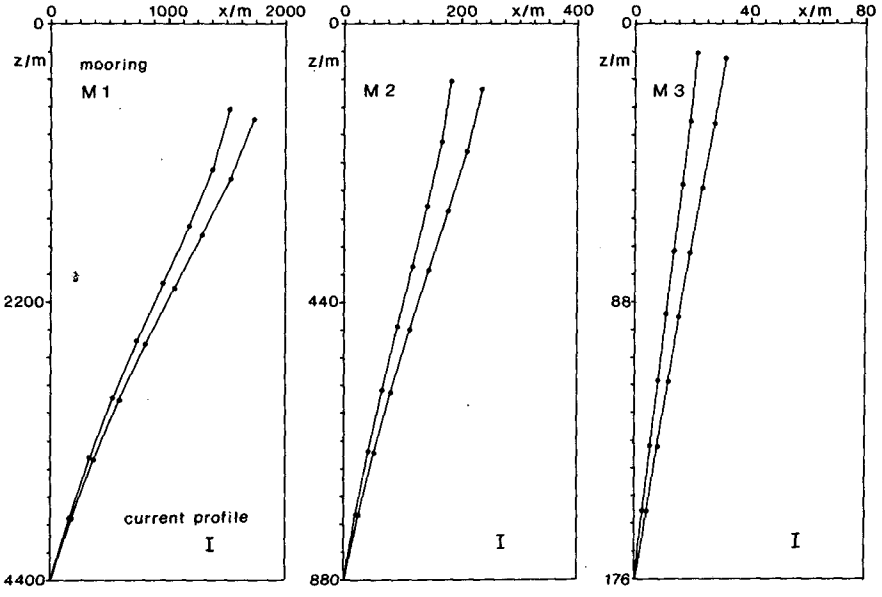


FIG. 12. Response of the three moorings M1–M3 to the linear current profile I with $C_D$ sets 1 (simple geometry, left curve) and 2 (data of this study, right curve).

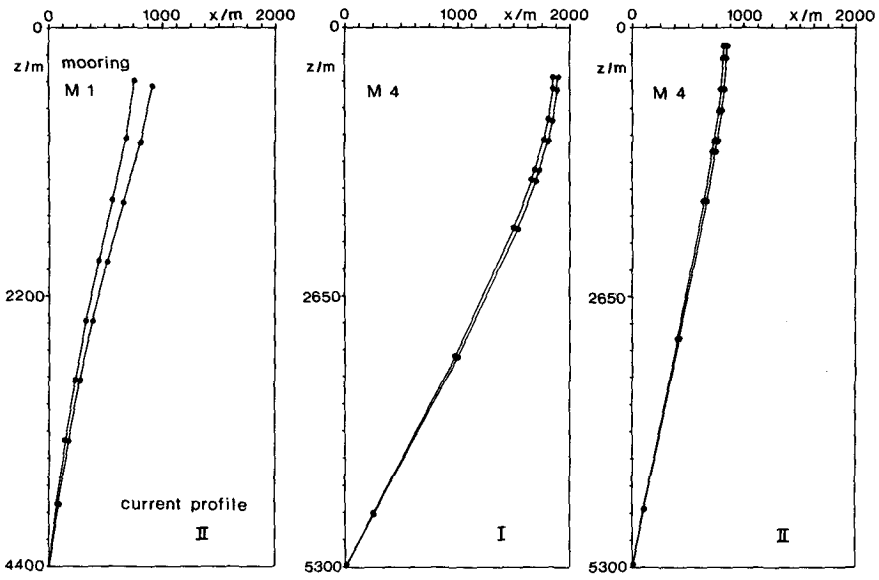


FIG. 13. Response of moorings M1 and M4 to selected current profiles with $C_D$ sets 1 (simple geometry, left curve) and 2 (data of this study, right curve).

the case of three-dimensional bodies limited in length this is no longer valid. We define normal and tangential drag coefficients $C_{DN}$ and $C_{DT}$ by

$$C_{DN} = \frac{2F_N}{\rho A V^2}, \tag{6}$$

$$C_{DT} = \frac{2F_T}{\rho A V^2}, \tag{7}$$

where $F_N$ and $F_T$ are the drag forces normal and tangential to the body's axis, $A$ is the cross-sectional area for the non-tilted case as defined in Eq. (1), and $V$ is the horizontal velocity. For the temperature recorder TR 1 the drag coefficients $C_{DN}$ and $D_{DT}$ based on normal and tangential drag force are shown in Fig. 9, indicating a dependence on the sine and cosine of the angle relative to flow direction. The tangential drag composes a considerable part of the total drag. Drag coefficients for the horizontal drag force according to Eq. (2) acting on the Kiel 450 kg Float K450 are presented in Fig. 10. A significant increase towards greater angles is found, and a similar dependence is assumed for the Benthos 2-ball buoyancy float B2. A comparison of drag coefficients for the mooring components tested is presented in Table 2.

## 5. Prediction of mooring performance

The effect of changing $C_D$ from the traditionally used simple shape values to the $C_D$ values obtained from our tow tank experiments will be studied in the following. In order to determine systematic differences between deep-sea and shallow-water moorings three sub-

TABLE 4. Depths $z$ and horizontal displacements $x$ of top components, and increases in depth $\Delta z$ and in displacement $\Delta x$ of top components with the change from $C_D$ set 1 (simple geometry) to set 2 (data of this study).

| Profile | Mooring | Depths (m) | | | Horizontal displacement (m) | | Change in: | |
|---|---|---|---|---|---|---|---|---|
| | | No drag | $C_D$ set 1 | $C_D$ set 2 | $C_D$ set 1 | $C_D$ set 2 | Depth (m) | Horizontal displacement (m) |
| I | M1 | 360.0 | 672.2 | 763.0 | 1530.6 | 1726.6 | 90.8 | 196.0 |
| | M2 | 67.5 | 88.9 | 103.4 | 183.3 | 236.1 | 14.5 | 52.8 |
| | M3 | 7.3 | 9.1 | 10.6 | 21.8 | 31.6 | 1.5 | 9.8 |
| II | M1 | 360.0 | 434.3 | 469.9 | 760.5 | 913.3 | 35.6 | 152.8 |
| I | M4 | 113.4 | 484.0 | 500.4 | 1855.0 | 1891.3 | 16.4 | 36.3 |
| II | M4 | 113.4 | 180.4 | 185.1 | 821.3 | 847.2 | 4.7 | 25.9 |
| III | M4 | 113.4 | 673.0 | 680.1 | 2330.2 | 2340.9 | 7.1 | 10.7 |

surface moorings with corresponding configurations and depth ratios 25:5:1 were selected (Fig. 11a).

M1: Deep-sea mooring, bottom depth 4400 m, top component at 360 m depth

M2: Medium-depth mooring, bottom depth 880 m, top component at 67.5 m depth

M3: Shallow-water mooring, bottom depth 176 m, top component at 7.3 m depth.

Corresponding configurations and current profiles are selected. Only Benthos glass spheres are used for providing buoyancy, eight current meters are included, and the ratio of total buoyancy to total weight in water was set constant for all three moorings. Cables are assumed to be cylindric with 11 mm diameter and a weight of 0.6 N $m^{-1}$. The values of $C_{DN}$ and $C_{DT}$ for normal and tangential drag forces are 1.3 and 0.007, respectively. The computer programs are taken from Schröder (1982) and Breitenbach and Schröder (1983), with appropriate changes of $C_D$. Two types of current profiles with constant direction are assumed for the moorings M1 to M3: A linear profile I with constant surface-to-bottom speed difference and a profile II which is similar to a case observed in the northeast Atlantic by Siedler et al. (1985). Also determined is the response of a mooring M4 (Fig. 11b) actually deployed by the above authors, with the profiles just mentioned and another case of an observed current profile (III). The profiles I–III are presented in Table 3.

The resulting mooring line configurations for the two sets of $C_D$ and current profiles no. I and II are presented in Figs. 12 and 13. Table 4 summarizes the increases in depth and displacement of the top component of all the moorings considered.

## 6. Discussion

In the seasonal and main thermocline of the ocean, vertical displacements of temperature sensors from a few to tens of meters will cause changes in the observed temperatures that are of similar order of magnitude as the temporal changes at a fixed level. Horizontal displacements cause errors in current observations due to the reduced velocity relative to the current sensor during the period the mooring needs to reach its equilibrium after a change in currents (Paquette, 1963). Since a certain amount of mooring inclination cannot be avoided, a knowledge of the actual displacements in a strong-current regime is required to estimate the above errors in time series observations. In order to predict changes in mooring inclination during the design phase, drag forces have to be calculated for expected current profiles. The tow tank experiments of this study yield the result that major deviations in drag coefficient values occur when comparing coefficients for mooring components to those of corresponding bodies with simple geometric shapes. Deviations are on the order of 10–50%.

The above deviations in drag coefficients cause an increase of horizontal and vertical mooring displacements. Although the total drag on the components discussed here will in general be small compared to the total drag on the cables, the deviations resulting from this study are not negligible. In extremely strong currents, the change in vertical displacement is about 10–100 m, in more typical open-ocean currents it is around 10 m. Such depth changes are sufficiently large to cause essential errors in temperature time series observation, and they can be important for current observations in the case of strong vertical current shear.

*Acknowledgments.* The Institut für Schiffbau of Hamburg University provided the tow tank facilities for this study. The assistance of the institute's staff, particularly of H. Keil and H. Thiemann, was much appreciated. The authors would also like to thank J. Breitenbach, then at the Institut für Meereskunde of Kiel University, for his help in planning and setting up the tow tank experiments. The study was partly funded by the Deutsche Forschungsgemeinschaft.

## REFERENCES

Berteaux, H. O., 1976: *Buoy Engineering.* Wiley-Interscience, 314 pp.

——, and R. G. Walden, 1967: Analysis and experimental evaluation of single point moored buoy systems. WHOI Tech. Rep. No. 69-36.

Breitenbach, J., and M. Schröder, 1983: Instruction manual for the computer program STASIP (statics of single point moorings). Ber. Inst. Meeresk., Universität Kiel, No. 109, 99 pp.

Casarella, M. J., and M. Parsons, 1970: Cable systems under hydrodynamic loading. *J. Mar. Technol. Soc.*, **4**, 27–44.

Choo, Y. I., and M. J. Casarella, 1971: Hydrodynamic Resistance of Towed Cables. *J. Hydronaut.*, **6**, 126–131.

Finke, M., 1984: Measurements of mooring component drag coefficients. Ber. Inst. Meeresk., Universität Kiel, No. 129, 96 pp.

Fofonoff, N. P., 1969: Buoy-system motions. *Handbook of Ocean and Underwater Engineering,* McGraw Hill, 9-109 to 9-115.

Hoerner, S. F., 1965: *Fluid Dynamic Drag.* Publ. by the Author, New Jersey.

Myers, D. A., C. H. Holm and R. F. McAllister, 1969: *Handbook of Ocean and Underwater Engineering.* McGraw Hill, 1-2 to 12-112 pp. + appendix.

Paquette, R. G., 1963: Practical problems in the direct measurement of ocean currents. *Marine Sciences Instrumentation, Vol. 2,* Instr. Soc. Amer., Plenum Press, 135–146.

Prandtl, L., 1969: Führer durch die Strömungslehre. Vieweg & Sohn, Braunschweig, 535 pp.

Sass, F., and Ch. Bouché, 1956: *Dubbels Taschenbuch für Maschinenbau,* Springer-Verlag, 884 pp.

Siedler, G., W. Zenk and W. J. Emery, 1985: Strong-current events related to a subtropical front in the Northeast Atlantic. *J. Phys. Oceanogr.*, **15**, 885–897.

Sigloch, H., 1982: *Technische Fluidmechanik.* VDI-Verlag, Düsseldorf, 328 pp.

Snyder, R. M., 1965: A practical Approach to Hydrodynamic Drag. *Geo-Mar. Technol.*, **1**(4), 33–37.

Schröder, M., 1982: The static behavior of single point moorings in currents. Ber. Inst. Meeresk., Universität Kiel, No. 108, 164 pp.